Article

Trivalent Polyhedra as Duals of Borane Deltahedra: From Molecular Endohedral Germanium Clusters to the Smallest Fullerenes

R. Bruce King

Department of Chemistry, University of Georgia, Athens, GA 30602, USA; rbking@uga.edu

Abstract: The duals of the most spherical *closo* borane deltahedra having from 6 to 16 vertices form a series of homologous spherical trivalent polyhedra with even numbers of vertices from 8 to 28. This series of homologous polyhedra is found in endohedral clusters of the group 14 atoms such as the endohedral germanium cluster anions $[M@Ge_{10}]^{3-}$ (M = Co, Fe) and $[Ru@Ge_{12}]^{3-}$. The next members of this series have been predicted to be the lowest energy structures of the endohedral silicon clusters $Cr@Si_{14}$ and $M@Si_{16}$ (M = Zr, Hf). The largest members of this series correspond to the smallest fullerene polyhedra found in the endohedral fullerenes $M@C_{28}$ (M = Zr, Hf, Th, U). The duals of the oblate (flattened) ellipsoidal deltahedra found in the dirhenaboranes $Cp^*_2Re_2B_{n-2}H_{n-2}$ ($Cp^* = \eta^5\text{-}Me_5C_5$; $8 \leq n \leq 12$) are prolate (elongated) trivalent polyhedra as exemplified experimentally by the germanium cluster $[Co_2@Ge_{16}]^{4-}$ containing an endohedral Co_2 unit.

Keywords: dualization of polyhedra; borane deltahedra; endohedral germanium clusters; small fullerenes

1. Introduction

The fundamental structural units for polyhedral boranes, including the $B_nH_n^{2-}$ dianions as well as the isoelectronic carboranes $CB_{n-1}H_n^-$ and $C_2B_{n-2}H_n$, are the most spherical *closo* deltahedra in which all of the faces are triangles (Table 1). [? ? ?] Such deltahedra are also the structural units for many other types of cluster compounds, including transition metal and post-transition element clusters. Thus bare group 14 element vertices (Si, Ge, Sn, Pb) as well as $Fe(CO)_3$ and $(\eta^5\text{-}C_5H_5)Co$ vertices are valence isoelectronic and isolobal with BH vertices. Similarly bare group 15 element vertices (P, As, Sb, Bi) vertices as well as $Co(CO)_3$ and $(\eta^5\text{-}C_5H_5)Ni$ vertices are valence isoelectronic and isolobal with CH vertices. The duals of these most spherical deltahedra represent a series of most spherical trivalent polyhedra in which the degree 3 vertices correspond to the triangular faces of the most spherical deltahedra. This paper surveys the wide range of cluster structures ranging from molecular endohedral germanium clusters to the smallest endohedral fullerenes based on trivalent polyhedra that are duals of the deltahedra found in polyhedral borane and metallaborane chemistry.

The most spherical *closo* deltahedra have the following features:

(1)   All faces are triangles—hence their designation as deltahedra relating to the shape of the Greek letter delta (Δ). This feature maximizes the number of edges for a given number of vertices and thus maximizes the connectivity between the vertices.

(2)   The vertices are as nearly similar as possible thereby providing the best approximation to a sphere rather than a prolate or oblate ellipsoid.

With these features in mind, the most spherical *closo* deltahedra can be classified into the following three types:

(3) Deltahedra with exclusively degree 4 and 5 vertices where the degree of a given vertex is the number of edges meeting at that vertex (Figure 1). These start with the highly symmetrical (O_h) 6-vertex regular octahedron with exclusively degree 4 vertices and go as far as the D_{4d} 10-vertex bicapped square antiprism with two degree 4 vertices and eight degree 5 vertices. These deltahedra are found in the borane dianions $B_nH_n{}^{2-}$ and the isoelectronic carboranes $CB_{n-1}H_n{}^-$ and $C_2B_{n-2}H_n$ [? ? ?].

(4) The four Frank-Kasper deltahedra [?] with exclusively degree 5 and degree 6 vertices with no pair of degree 6 vertices sharing an edge (Figure 2). These start with the highly symmetrical (I_h) 12-vertex regular icosahedron and also include the 14-vertex D_{6d} bicapped hexagonal antiprism with antipodal degree 6 vertices, a 15-vertex D_{3h} deltahedron with its three degree 6 vertices forming an equilateral macrotriangle, and the 16-vertex T_d tetracapped tetratruncated tetrahedron with its four degree 6 vertices forming a regular macrotetrahedron. The icosahedral structure is found in the borane dianion $B_{12}H_{12}{}^{2-}$ as well as the isoelectronic carboranes $CB_{11}H_{12}{}^-$ and $C_2B_{10}H_{12}$ [? ? ?]. The 14-vertex bicapped hexagonal antiprism is found in (μ-CH_2)$_3C_2B_{12}H_{12}$ in which the two carbon vertices are bridged by a trimethylene unit [?]. The 16-vertex tetracapped tetratruncated tetrahedron is found in the unusual pentarhodium complex (Cp^*Rh)$_3B_{12}H_{12}Rh(B_4H_9\ RhCp^*$) ($Cp^*$ = η^5-Me_5C_5) [?].

(5) For the 11- and 13-vertex systems the *closo* deltahedra are less symmetrical and necessarily contain vertices of three different degrees, namely 4, 5, and 6 (Figure 3).
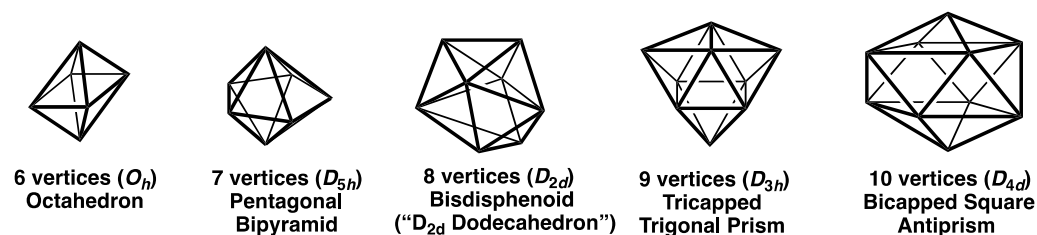

6 vertices (O_h)
Octahedron

7 vertices (D_{5h})
Pentagonal
Bipyramid

8 vertices (D_{2d})
Bisdisphenoid
("D_{2d} Dodecahedron")

9 vertices (D_{3h})
Tricapped
Trigonal Prism

10 vertices (D_{4d})
Bicapped Square
Antiprism

Figure 1. The most spherical *closo* polyhedra having 6 to 10 vertices.

12 vertices (I_h)
Icosahedron

14 vertices (D_{6d})
Bicapped hexagonal
antiprism

15 vertices (D_{3h})

16 vertices (T_d)
Tetracapped
Tetratruncated
Tetrahedron
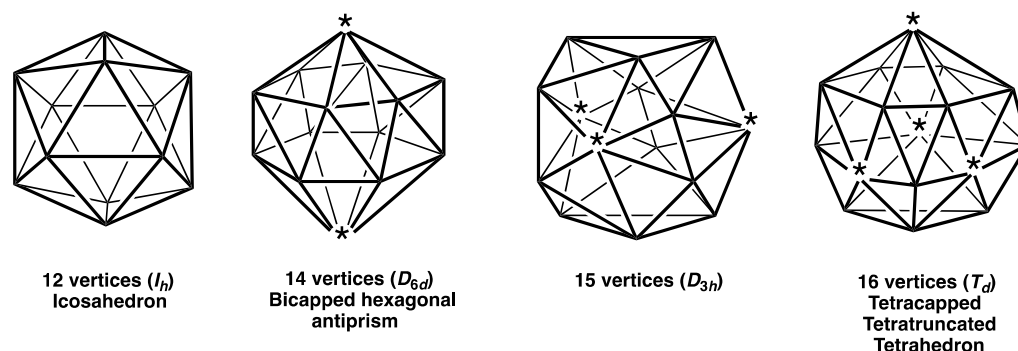
Figure 2. The four Frank-Kasper deltahedra with the degree 6 vertices starred.
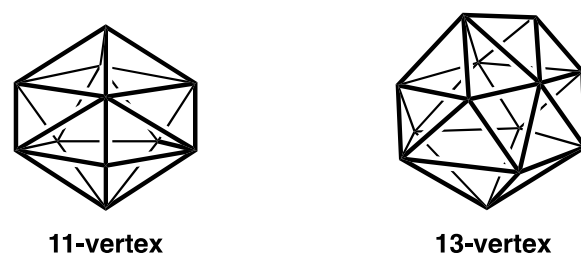

11-vertex

13-vertex

Figure 3. The 11- and 13-vertex *closo* deltahedra.

The 16-vertex Frank-Kasper deltahedron is a natural upper limit to the number of vertices in this homologous series of most spherical deltahedra. Thus deltahedra having more than 16 vertices require adjacent degree 6 vertices and/or vertices of degrees higher

than 6. Adjacent degree 6 vertices lead to "flat spots" on the surface of the deltahedron and vertices of degrees higher than 6 can even lead to indentations ("negative curvature") on the polyhedral surface. Either of these features leads to significant distortion from sphericity.

The initially synthesized group 14 element clusters containing interstitial atoms have deltahedral structures for the outer group 14 shell. Thus in the trianions $[Cu@E_9]^{3-}$ (E = Sn, Pb) a copper atom is encapsulated by a *closo* 9-vertex tricapped trigonal prismatic tin or lead cluster [?]. Similarly, the *closo* 10-vertex D_{4h} bicapped square antiprism encapsulating a metal atom was found to be the structural motif for the anionic indium cluster $Zn@In_{10}^{8-}$ found in the intermetallic [?] $K_8In_{10}Zn$ as well as in the lead clusters $M@Pb_{10}^{2-}$ found in $[K(2,2,2\text{-crypt})]_2[M@Pb_{10}]$ (M = Ni, Pd, Pt). [? ?] The other 10-vertex polyhedra, such as the C_{3v} tetracapped trigonal prism in the $M@Ga_{10}^{10-}$ clusters found in the $K_{10}Ga_{10}M$ intermetallics (M = Ni, Pd, Pt) [?] and the pentagonal antiprism in the cationic bismuth cluster $Pd@Bi_{10}^{4+}$ in $Bi_{14}PdBr_{16}$ (=$[Pd@Bi_{10}][BiBr_4]_4$), [?] have all or at least mostly triangular faces. The dianion $[Pt@Pb_{12}]^{2-}$ contains a platinum atom encapsulated in a *closo* regular icosahedron of lead atoms. [?]

In view of these considerations the discovery of an outer Ge_{10} pentagonal prism in the anion $Co@Ge_{10}^{3-}$ of $[K(2,2,2\text{-crypt})]_4[Co@Ge_{10}][Co(1,5\text{-}C_8H_{12})_2]\bullet$toluene [?] and in the anion $Fe@Ge_{10}^{3-}$ of $[K(2,2,2\text{-crypt})]_3[Fe@Ge_{10}]$ [?] was a major surprise. Not only is the pentagonal prism not a most spherical deltahedron or even any kind of deltahedron, it does not have any triangular faces at all. I now show how the pentagonal prism, as the dual of the pentagonal bipyramid, is the second member of a homologous series of trivalent polyhedra starting with the cube and ending with the T_d 28-vertex polyhedron found in the endohedral fullerenes $M@C_{28}$ (M = Zr, Th, U). [?] In this connection, a trivalent polyhedron is defined as a polyhedron in which all vertices have degree 3. Such trivalent polyhedra must necessarily have an even number of vertices as well as the minimum number of edges for a polyhedron with a given number of vertices. Minimizing the number of edges for a given number of vertices maximizes the internal volume of the polyhedron by minimizing the connectivity between the vertices. Therefore, trivalent polyhedra are especially suitable as maximum-volume containers for interstitial atoms.

In addition to the most spherical borane deltahedra (Table 1 and Figure 1) oblate (flattened) ellipsoidal deltahedra are found in the so-called *oblatocloso* dirhenaboranes $Cp*_2Re_2B_{n-2}H_{n-2}$ ($Cp* = \eta^5\text{-}Me_5C_5$; $8 \leq n \leq 12$) (Figure 4). [? ? ? ?] The flattened shape of these deltahedra arises from the need to bring the two rhenium atoms in approximately antipodal positions close enough to form a rhenium-rhenium bond through the center of the deltahedron. [?] The duals of such oblate deltahedra are prolate elongated trivalent polyhedra such as the 16-vertex polyhedron found experimentally in the germanium cluster $[Co_2@Ge_{16}]^{4-}$ with an endohedral Co_2 unit. [? ?]
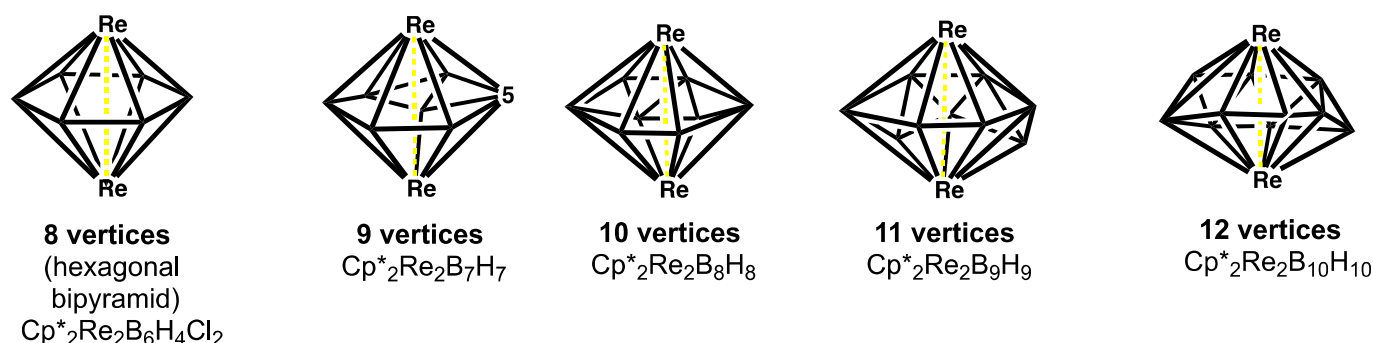

Figure 4. The oblate ellipsoidal (*oblatocloso*) deltahedra found in the dirhenaboranes $Cp*_2Re_2B_{n-2}H_{n-2}$ ($Cp* = \eta^5\text{-}Me_5C_5$; $8 \leq n \leq 12$).

2. Dualization of Polyhedra

The dual of a polyhedron has its vertices located at the midpoints of the faces of the original polyhedron. Two vertices of the dual are connected by an edge if the corresponding

faces of the original polyhedron share an edge. The dualization of a polyhedron preserves the symmetry of the original polyhedron. Furthermore, the dualization of the dual of a polyhedron leads back to the original polyhedron. In this sense, the process of dualization has a period of two so that polyhedra occur in natural pairs of a given polyhedron and its dual. Among the five regular polyhedra the octahedron and cube form a dual pair exhibiting O_h symmetry and the icosahedron and dodecahedron form a dual pair exhibiting I_h symmetry. The tetrahedron is a self-dual polyhedron since the dual of a tetrahedron is another tetrahedron. Self-dual polyhedra necessarily have the same number of vertices and faces. In this connection, pyramids are self-dual polyhedra. The dual of a bipyramid is a prism of the same symmetry and vice versa. The dual of an antiprism is a trapezohedron of the same symmetry and vice versa,

A number of chemically significant polyhedra are derived by capping one or more faces of smaller polyhedra. Examples among the most spherical *closo* deltahedra include the 9-vertex D_{3h} tricapped trigonal prism and the 10-vertex D_{4d} bicapped square antiprism (Figure 1). The dual process of capping is truncation (Figure 5). Truncation consists of cutting off a vertex to generate a new polygonal face with a number of sides corresponding to the degree of the cut-off vertex. Thus the dual of the D_{3h} tricapped trigonal prism is the 14-vertex tritruncated trigonal bipyramid, also of D_{3h} symmetry. Similarly, the dual of the D_{4d} bicapped square antiprism is the bitruncated square trapezohedron, also of D_{4d} symmetry. Dualization of the 16-vertex tetracapped tetratruncated tetrahedron, namely the 16-vertex Frank Kasper deltahedron (Figure 2), gives the tetratruncated tetracapped tetrahedron. In this case, dualization consists of reversing the order of tetracapping and tetratruncating the original tetrahedron.
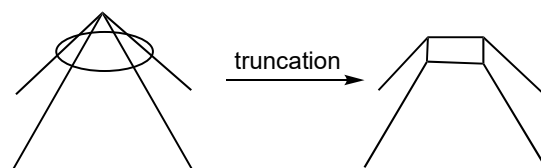

Figure 5. Schematic representation of the truncation of a degree 4 vertex to give a new tetragonal face.

3. The Most Spherical Trivalent Polyhedra in Chemistry

The duals of the most spherical *closo* deltahedra form a natural series of most spherical maximum volume trivalent polyhedra starting with the 8-vertex cube and ending with the 28-vertex tetratruncated tetracapped tetrahedron (Table 1). The duals of the 6- to 10-vertex *closo* deltahedra (Figure 1) have exclusively tetragonal and pentagonal faces (Figure 6). Similarly, the duals of the four Frank-Kasper deltahedra (Figure 2) have exclusively pentagonal and hexagonal faces (Figure 7). The duals of the less symmetrical and thus less distinctive 11- and 13-vertex *closo* deltahedra (Figure 3) necessarily have three different types of faces, namely tetragonal, pentagonal, and hexagonal faces. They have not been identified in any chemical structures and thus are not discussed in this paper.
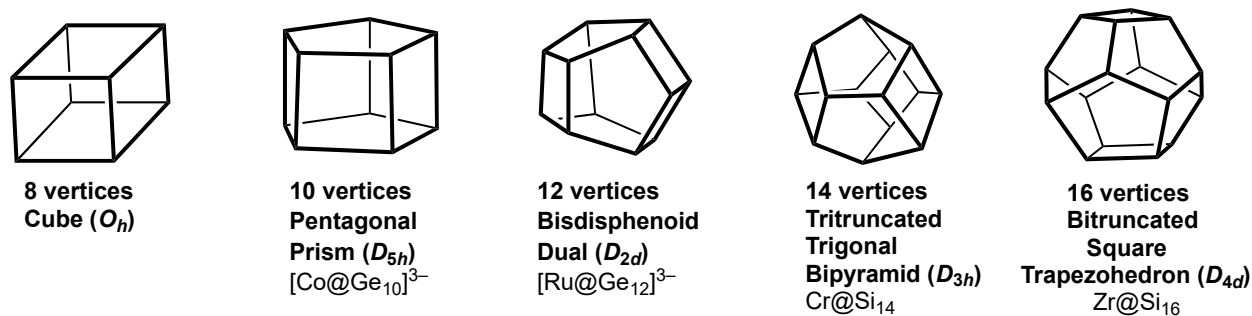

8 vertices
Cube (O_h)

10 vertices
Pentagonal
Prism (D_{5h})
$[Co@Ge_{10}]^{3-}$

12 vertices
Bisdisphenoid
Dual (D_{2d})
$[Ru@Ge_{12}]^{3-}$

14 vertices
Tritruncated
Trigonal
Bipyramid (D_{3h})
$Cr@Si_{14}$

16 vertices
Bitruncated
Square
Trapezohedron (D_{4d})
$Zr@Si_{16}$

Figure 6. The most spherical trivalent polyhedra with 8, 10, 12, 14, and 16 vertices as duals of the *closo* deltahedra in endohedral Group 14 clusters.
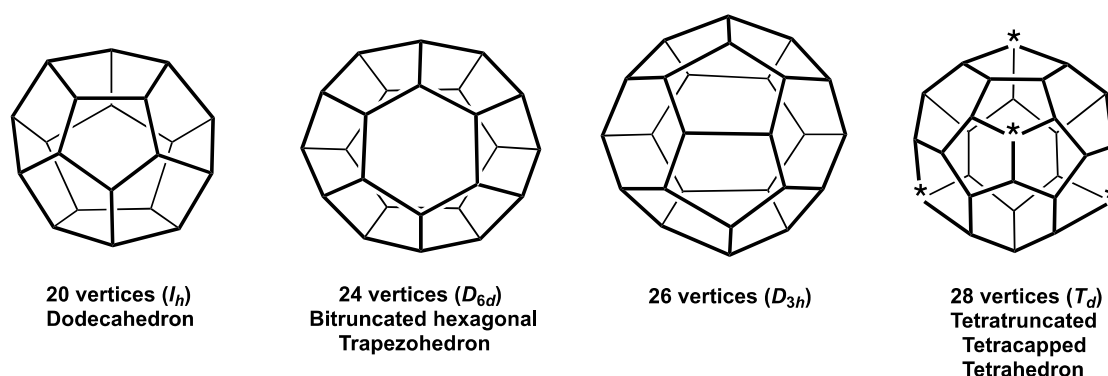
Figure 7. The most spherical trivalent polyhedra having 20, 24, 26, and 28 vertices as duals of the Frank-Kasper deltahedra (Figure 2). In the T_d 28-vertex polyhedron the four degree 3 vertices each shared by three pentagonal faces are starred to indicate their orientation in M@C_{28} species.

The group 14 elements (C, Si, Ge, Sn, Pb) are well suited to be vertices of trivalent polyhedra. The four tetrahedrally disposed sp^3 orbitals of each group 14 element vertex allow for three two-center two-electron bonds along each of the polyhedral edges connected to that vertex leaving an external sp^3 hybrid for a lone pair. The maximum volume feature of the most spherical trivalent polyhedra is important in order to have a large enough cavity to accommodate an interstitial atom. The smallest members of the trivalent polyhedral homologous series allow germanium clusters to accommodate an interstitial transition metal atom. This is where the pentagonal prismatic [M@Ge_{10}]$^{3-}$ (M = Co, [?] Fe [?]) trianions fit into the picture. Similarly the 12-vertex bisdisphenoid dual is found in the [Ru@Ge_{12}]$^{3-}$ trianion found in [K(2,2,2-crypt)]$_3$[Ru@Ge_{12}]·4py [? ?] and in the anion [Ta@Ge_8As_4]$^{3-}$, also found in a [K(2,2,2-crypt)]$^+$ salt of more complicated stoichiometry [?]. The larger 14-vertex tritruncated trigonal bipyramid is found in the lanthanide-centered [Ln@Sn_7Bi_7]$^{4-}$ (Ln = La, Ce) tetraanions [?] and is predicted to be a favorable polyhedron for M@Si_{14} clusters encapsulating first row transition metals, some of which are observed in supersonic beams [?]. The 16-vertex bitruncated square trapezohedron is also found as a silicon cluster encapsulating a heavier group 4 metal atom in low energy M@Si_{16} (M = Zr, Hf) structures [? ? ?].

The most spherical trivalent polyhedra with 20 or more vertices correspond to the smallest C_n fullerenes having only pentagonal and hexagonal faces. Even with carbon vertices, such polyhedra become large enough to encapsulate metal atoms. Thus the 28-vertex tetratruncated tetracapped tetrahedron (Figure 6) can accommodate group 4 metals and actinides in the M@C_{28} species (M = Zr, Th, U) [?]. In these structures the tetrahedral orientation of the four vertices common to three fused pentagonal rings (starred vertices in Figure 6) provide tetrahedral coordination for the encapsulated metal atom.

The M@C_{28} (M = Zr, Th, U) species are the smallest fullerene derivatives that have been realized experimentally. However, the endohedral fullerenes U@C_{26} exhibiting the D_{3h} most spherical trivalent polyhedral geometry [?] and Pu@C_{24} exhibiting D_{6d} bitruncated hexagonal trapezohedral geometry [?] (Figure 7) are predicted to be favorable species with high HUMO-LUMO gaps and positive binding energies. The endohedral silicon cluster anion [U@Si_{20}]$^{6-}$ with an outer Si_{20} regular (I_h) dodecahedron (Figure 6) is also predicted to be a favorable species by similar criteria [?]. All of these favorable endohedral clusters with geometries based on duals of the Frank-Kasper polyhedra (Figure 6) have 32 skeletal electrons (= $2n^2$ for $n = 4$) counting one skeletal electron for each group 14 element vertex and all of the valence electrons of the endohedral atom. This relates to the spherical aromaticity [?] of such systems consisting of filled 1S + 1P + 1D + 1F molecular orbitals leaving a significant HOMO-LUMO gap.

Table 1. The most spherical *closo* deltahedra and their duals.

Vertices/ Faces (Dual)	Edges	Faces/ Vertices (Dual)	*Closo Deltahedron* (Symmetry)	Dual Trivalent Polyhedron	Chemical Example of Dual [a] [lit. ref.]
6	12	8	Octahedron (O_h)	Cube	
7	15	10	Pentag bipyramid (D_{5h})	Pentag prism	$[Co@Ge_{10}]^{3-}$ [?]
8	18	12	Bisdisphenoid (D_{2d})		$[Ru@Ge_{12}]^{3-}$ [?]
9	21	14	Tricap trig prism (D_{3h})	Tritrunc trig bipyramid	$Cr@Si_{14}$ [?]
10	24	16	Bicap sq antiprism (D_{4d})	Bitrunc sq trapezohedron	$Zr@Si_{16}$ [? ? ?]
11	27	18	(C_{2v})		
12	30	20	Icosahedron (I_h)	Dodecahedron	$\{[U@Si_{20}]^{6-}\}$ [?]
13	33	22			
14	36	24	Bicap hex antiprism (D_{6d})	Bitrunc hex trapezohedron	$\{Pu@C_{24}\}$ [?]
15	39	26	15v Frank Kasper (D_{3h})		$\{U@C_{26}\}$ [?]
16	42	28	Tetracap tetratrunc tet (T_d)	Tetratrunc tetracap tet	$Th@C_{28}$ [?]

[a] Species predicted theoretically but not yet realized experimentally are listed in braces {}. Literature references are indicated in brackets [].

4. Prolate Elongated Ellipsoidal Trivalent Polyhedra as Duals of Oblate Flattened Ellipsoidal Deltahedra

The series of hypoelectronic dirhenaboranes $Cp^*_2Re_2B_{n-2}H_{n-2}$ ($Cp^* = \eta^5\text{-}Me_5C_5$; $8 \leq n \leq 12$) have central oblate (flattened) ellipsoidal Re_2B_{n-2} deltahedra (Figure 4) that are very different from the most spherical *closo* borane deltahedra (Figure 1) [? ? ?]. The flattening arises from the need to bring the two approximately antipodal rhenium atoms close enough (2.69 to 2.94 Å) for a direct Re=Re interaction through the center of the deltahedron [?].

Dualization of an oblate (flattened) ellipsoidal deltahedron such as those found in the hypoelectronic dirhenaboranes leads to a prolate (elongated) trivalent polyhedron. The elongated shapes and relatively large internal volumes of such prolate trivalent polyhedra make them particularly suitable to incorporate a pair of interstitial metal atoms. This is seen experimentally in the $[Co_2@Ge_{16}]^{4-}$ tetraanion found in the salt $[K(2,2,2\text{-crypt})]_4[Co_2@Ge_{16}]\cdot en$ where one of the two isolated and crystallographically characterized isomers has a structure based on a prolate trivalent polyhedron with two hexagonal faces, four pentagonal faces, and four tetragonal faces (Figure 8) [? ?]. The Co–Co distance of 2.75 Å in the endohedral Co_2 unit of this structure can correspond to a long single bond. This prolate trivalent polyhedron bears an approximate dual relationship with the oblate deltahedron found in the dirhenaborane $Cp^*_2Re_2B_8H_8$ with two vertices of degree 6, four vertices of degree 5, and two vertices of degree 6. In this case, the duality relationship is not exact since there is a shift of the relative positions of the four degree 5 and four degree vertices in the $Cp^*_2Re_2B_8H_8$ structure in order to place the pair of rhenium atoms at the optimum distance for the intrapolyhedral rhenium-rhenium bonding.
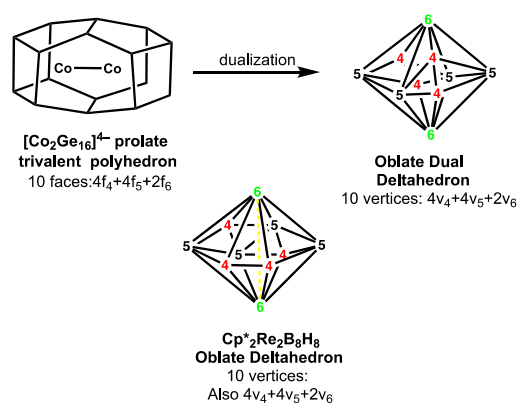

Figure 8. Dual relationship between the 16-vertex prolate ellipsoidal trivalent polyhedron in $[Co_2Ge_{16}]^{4-}$ and the 10-vertex oblate ellipsoidal deltahedron in $Cp^*_2Re_2B_8H_8$.

5. Conclusions

The duals of the most spherical *closo* borane deltahedra having from 6 to 16 vertices form a series of homologous spherical trivalent polyhedra having even numbers of vertices from 8 to 28. This series of homologous polyhedra is found in endohedral clusters of the group 14 atoms. Thus the smallest members of this series are found in the endohedral germanium cluster anions $[M@Ge_{10}]^{3-}$ (M = Co, Fe) and $[Ru@Ge_{12}]^{3-}$ with D_{5h} pentagonal prism and D_{2d} bisdisphenoid dual geometries, respectively. The next members of this series have been predicted to be the lowest energy structures of the endohedral silicon clusters $Cr@Si_{14}$ and $M@Si_{16}$ (M = Zr, Hf) with D_{3h} tritruncated trigonal bipyramid and D_{4d} bitruncated tetragonal trapezohedron geometries, respectively. The largest members of this series correspond to the smallest fullerene polyhedra. The last member of this series, namely the T_d tetratruncated tetracapped tetrahedron dual to the 16-vertex Frank-Kasper deltahedron, is found in the endohedral fullerenes $M@C_{28}$ (M = Zr, Hf, Th, U), which are the smallest fullerene polyhedra known experimentally. Thus the homologous series of most spherical trivalent polyhedra represent a transition from molecular endohedral clusters of the heavier group 14 elements to the smallest fullerene derivatives. In addition, the duals of the oblate (flattened) ellipsoidal deltahedra found in the dirhenaboranes $Cp^*_2Re_2B_{n-2}H_{n-2}$ ($Cp^* = \eta^5\text{-Me}_5C_5$; $8 \leq n \leq 12$) are prolate (elongated) trivalent polyhedra as exemplified experimentally by the germanium cluster $[Co_2@Ge_{16}]^{4-}$ with an endohedral Co_2 unit.

References

1. Williams, R.E. Carboranes and boranes; polyhedral and polyhedral fragments. *Inorg. Chem.* **1971**, *10*, 210–214. [CrossRef]
2. Williams, R.E. The polyborane, carborane, carbocation continuum: Architectural patterns. *Chem. Rev.* **1992**, *92*, 177–207. [CrossRef]
3. King, R.B. Three-dimensional aromaticity in polyhedral boranes and related molecules. *Chem. Rev.* **2001**, *101*, 1119–1152. [CrossRef]
4. Frank, F.C.; Kasper, J.S. Complex alloy structures regarded as sphere packings. 1. Definitions and basic principles. *Acta Cryst.* **1958**, *11*, 184–190. [CrossRef]
5. Dong, L.; Chen, H.S.; Xie, Z. Synthesis, reactivity, and structural characterization of a 14-vertex carborane. *Angew. Chem. Int. Ed. Engl.* **2005**, *44*, 2128–2131. [CrossRef]
6. Roy, S.K.; Mondal, B.; Shankhari, P.; Anju, R.S.; Geetharani, K.; Mobin, S.M.; Ghosh, S. Supraicosahedral polyhedra in metallaboranes: Synthesis and structural characterization of 12-, 15-, and 16-vertex rhodaboranes. *Inorg. Chem.* **2013**, *52*, 6705–6712. [CrossRef]
7. Scharfe, S.; Fässler, T.F.; Stegmaier, S.; Hoffmann, S.D.; Klaus, R. $[Cu@Sn_9]^{3-}$ and $[Cu@Pb_9]^{3-}$: Intermetalloid clusters with endohedral Cu atoms in spherical environments. *Chem. Eur. J.* **2008**, *14*, 4479–4483. [CrossRef]
8. Sevov, S.C.; Corbett, J.C. $K_8In_{10}Zn$—Interstitially stabilized analogs of early-transition metal halide clusters. *Inorg. Chem.* **1993**, *32*, 1059–1061. [CrossRef]
9. Esenturk, E.N.; Fettinger, J.; Eichhorn, B. The *closo*-Pb_{10}^{2-} Zintl ion in the $[Ni@Pb_{10}]^{2-}$ cluster. *Chem. Commun.* **2005**, 247–249. [CrossRef]
10. Esenturk, E.N.; Fettinger, J.; Eichhorn, B. The Pb_{12}^{2-} and Pb_{10}^{2-} Zintl ions and the $M@Pb_{12}^{2-}$ and $M@Pb_{10}^{2-}$ cluster series where M = Ni, Pd, Pt. *J. Am. Chem. Soc.* **2006**, *128*, 9178–9186. [CrossRef]
11. Henning, R.W.; Corbett, J.D. Formation of isolated nickel-centered gallium clusters in $Na_{10}Ga_{10}Ni$ and a 2-D network of gallium octahedra in K_2Ga_3. *Inorg. Chem.* **1999**, *38*, 3883–3888. [CrossRef]
12. Ruck, M.; Dubenskyy, V.; Söhnel, T. Structure and bonding of $[Pd@Bi_{10}]^{4+}$ in the subbromide $Bi_{14}PdBr_{16}$. *Angew. Chem. Int. Ed.* **2003**, *45*, 2978–2982. [CrossRef]
13. Esenturk, E.N.; Fettinger, J.; Lam, Y.-F.; Eichhorn, B. $[Pt@Pb_{12}]^{2-}$. *Angew. Chem. Int. Ed.* **2004**, *43*, 2132–2134. [CrossRef]
14. Wang, J.-Q.; Stegmaier, S.; Fässler, T.F. $[Co@Ge_{10}]^{3-}$: An intermetalloid cluster with Archimedean pentagonal prismatic structure. *Angew. Chem. Int. Ed.* **2009**, *48*, 1998–2002. [CrossRef]

15. Zhou, B.; Denning, M.S.; Kays, D.L.; Goicoechea, J.M. Synthesis and isolation of [Fe@Ge$_{10}$]$^{3-}$: A pentagonal prismatic Zintl ion cage encapsulating an interstitial iron atom. *J. Am. Chem.Soc.* **2009**, *132*, 2802–2803. [CrossRef]

16. Dunk, P.W.; Kaiser, N.K.; Mulet-Gas, M.; Rodriguez-Fortea, A.; Poblet, J.M.; Shinohara, H.; Hendrickson, C.L.; Marshall, A.G.; Kroto, H.W. The smallest stable fullerene, M@C$_{28}$ (M = Ti, Zr, U): Stabilization and growth from carbon vapor. *J. Am. Chem. Soc.* **2012**, *134*, 9308–9389. [CrossRef]

17. For a review of much of the relevant chemistry from Fehlner's group see Fehlner, T. P. In *Group 13 Chemistry: From Fundamentals to Applications*; Shapiro, P.J.; Atwood, D.A. (Eds.) American Chemical Society: Washington, DC, USA, 2002; pp. 49–67.

18. Ghosh, S.; Shang, M.; Li, Y.; Fehlner, T.P. Synthesis of [(Cp*Re)$_2$B$_n$H$_n$] (*n* = 8–10): Metal boride particles that stretch the cluster structure paradigms. *Angew. Chem. Int. Ed.* **2001**, *40*, 1125–1128. [CrossRef]

19. Wadepohl, H. Hypoelectronic dimetallaboranes. *Angew. Chem. Int. Ed.* **2002**, *41*, 4220. [CrossRef]

20. Le Guennic, B.; Jiao, H.; Kahlal, S.; Saillard, J.-Y.; Halet, J.-F.; Ghosh, S.; Shang, M.; Beatty, A.M.; Rheingold, A.L.; Fehlner, T.P. Synthesis and characterization of hypoelectronic rhenaboranes. analysis of the geometric and electronic structures of species following neither borane nor metal cluster electron-counting paradigms. *J. Am. Chem. Soc.* **2004**, *126*, 3203–3217. [CrossRef] [PubMed]

21. King, R.B. The oblate deltahedra in dimetallaboranes: Geometry and chemical bonding. *Inorg. Chem.* **2006**, *45*, 8211–8216. [CrossRef]

22. Jin, X.; Espionoza-Quintero, G.; Below, B.; Arcisauskaite, V.; Goicoechea, J.M.; McGrady, J.E. Structure and bonding in a bimetallic endohedral cage, [Co$_2$@Ge$_{16}$]$^{2-}$. *J. Organometal. Chem.* **2015**, *792*, 149–153. [CrossRef]

23. Liu, C.; Popov, I.A.; Li, L.-J.; Li, N.; Boldyrev, A.I.; Sun, Z.-M. [Co$_2$@Ge$_{16}$]$^{4-}$: Localized versus delocalized bonding in two isomeric intermetalloid clusters. *Chem. Eur. J.* **2018**, *24*, 699–705. [CrossRef]

24. Espinoza-Qunitero, G.; Duckworth, J.C.A.; Myers, W.K.; McGrady, J.E.; Goicoechea, J.M. Synthesis and characterization of [Ru@Ge$_{12}$]$^{3-}$: An endohedral 3-connected cluster. *J. Am. Chem. Soc.* **2014**, *136*, 1210–1213. [CrossRef]

25. Goicoechea, J.M.; McGrady, J.E. On the structural landscape in endohedral silicon and germanium clusters, M@Si$_{12}$ and M@Ge$_{12}$. *Dalton Trans.* **2015**, *44*, 6755–6766. [CrossRef]

26. Mitzinger, S.; Broeckaert, L.; Massa, W.; Wiegend, F.; Dehnen, S. Understanding of multimetallic cluster growth. *Nat. Commun.* **2016**, *7*, 10480. [CrossRef]

27. Lips, F.; Holyńska, M.; Clérac, R.; Linne, U.; Schellenberg, I.; Pöttgen, R.; Weigend, F. Dehnen, S. Doped semimetal clusters: Ternary intermetalloid anions [Ln@Sn$_7$Bi$_7$]$^{4-}$ and [Ln@Sn$_4$Bi$_9$]$^{4-}$ (Ln = La, Ce) with adjustable magnetic properties. *J. Am. Chem. Soc.* **2012**, *134*, 1181–1191. [CrossRef]

28. Jin, X.; Arcisauskaite, V.; McGrady, J. The structural landscape in 14-vertex clusters of silicon, M@Si$_{14}$: When two bonding paradigms collide. *Dalton Trans.* **2017**, *46*, 11636–11644. [CrossRef]

29. Kumar, V. Novel metal-encapsulated caged clusters of silicon and germanium. *Eur. Phys. J. D* **2003**, *24*, 227–232. [CrossRef]

30. Kumar, V. Recent theoretical progress on electronic and structural properties of clusters: Permanent electric dipoles, magnetism, novel caged structures, and their assemblies. *Comput. Mater. Sci.* **2006**, *35*, 375–381. [CrossRef]

31. Kumar, V.; Majumder, C.; Kawazoe, Y. M@Si$_{16}$, M = Ti, Zr, Hf: π conjugation, ionization potentials and electron affinities. *Chem. Phys. Lett.* **2002**, *363*, 319–322. [CrossRef]

32. Manna, D.; Ghanty, T.K. Prediction of a new series of thermodynamically stable actinide encapsulated fullerene systems fulfilling the 32-electron principle. *J. Phys. Chem. C* **2012**, *116*, 25630–25641. [CrossRef]

33. Manna, D.; Sirohiwal, A.; Ghanty, T.K. Pu@C$_{24}$: A new example satisfying the 32-electron principle. *J. Phys. Chem. C* **2014**, *118*, 7211–7221. [CrossRef]

34. Dognon, J.-P.; Clavaguéra, C.; Pyykkö, P. A new, centered 32-electron system: The predicted [U@Si$_{20}$]$^{6-}$-like isoelectronic series. *Chem. Sci.* **2012**, *3*, 2843–2848. [CrossRef]

35. Bühl, M.; Hirsch, A. Spherical aromaticity of fullerenes. *Chem. Rev.* **2001**, *101*, 1153–1184. [CrossRef]